On-line calibration for linear time-base error correction of terahertz spectrometers with echo pulses

To cite this article: Yuqiang Deng *et al* 2014 *Metrologia* **51** 18

View the article online for updates and enhancements.

On-line calibration for linear time-base error correction of terahertz spectrometers with echo pulses

Yuqiang Deng, Qing Sun and Jing Yu

Optics Division, National Institute of Metrology, Beijing 100013, People's Republic of China

E-mail: yqdeng@nim.ac.cn

Abstract

We use a terahertz echo pulse as a transfer standard to correct linear time-base errors of a terahertz spectrometer. With this calibration technique, the linear error of the translate stage is corrected and the spectral repeatability of the spectrometer is improved. This calibration technique is able to correct each 'shot' of the terahertz pulse and can realize on-line calibration of the terahertz spectrum. The average of multiple measurements of carbon monoxide gas absorption lines was corrected and the deviation was reduced by a factor of 2.5 using this technique. This on-line calibration technique needs no additional optical components and causes no performance degradation of the terahertz spectrometer. It provides a simple and alternative method to the conventional interferometric technique and allows for accurate measurement of spectral properties of specimens in the terahertz region.

Keywords: metrological applications, optical frequency synthesizers for precision spectroscopy, infrared sources, optical elements, devices, and systems

(Some figures may appear in colour only in the online journal)

1. Introduction

Terahertz (THz) radiation provides powerful insights into the material properties of biological specimens, chemical drugs and explosive goods that cannot be accessed otherwise [1, 2]. Therefore, a THz spectrometer becomes an attractive tool for diverse applications, including medical analysis and biochemical stand-off detection for hazardous materials [3]. Accurate characterization of fingerprint spectra is necessary in most of these applications [4]. Therefore, calibration of THz spectrometers is unavoidable and thus receives considerable attention [5, 6]. The absorption spectral lines of water vapour have been taken as a standard for THz frequency calibration ever since they were measured by van Exter *et al* [5, 7]. However, the spectral lines of water vapour are doublets and triplets, and they vary with environmental conditions [7], especially for different humidities [8]. Therefore, this calibration may lead to a mismatch of spectral lines.

Carbon monoxide (CO) gas provides a train of comb-like clear absorption lines in the THz range [6, 9]. These narrow absorption lines are equally spaced in the frequency domain and possess a characteristic amplitude envelope. Naftaly *et al* employed a CO gas cell as a standard for high-resolution THz frequency calibration [6]. CO gas has a series of equally spaced absorption lines; with this technique, therefore, the risk of mismatch of spectral lines calibrated with water vapour is avoided. The sharp and narrow absorption peaks of CO allow this calibration technique to have a frequency resolution as high as 2 GHz [6]. With this kind of calibration technique, however, calibration and actual measurement cannot be performed at the same time. Therefore, the measurement error generated from the instrument unrepeatability cannot be corrected. The unrepeatability may be generated from the control software, the translation stage itself and the measurement conditions, such as temperature and humidity. This especially concerns the so-called 'open-loop technique', in which the translation stage runs with a constant speed and the time-domain waveform is recorded according to the relationship between the time coordinate and the translation speed. In some THz spectrometers, the frequency unrepeatability may be as large as 4 GHz, which we will demonstrate in a practical measurement. Therefore, accurate calibration with CO gas
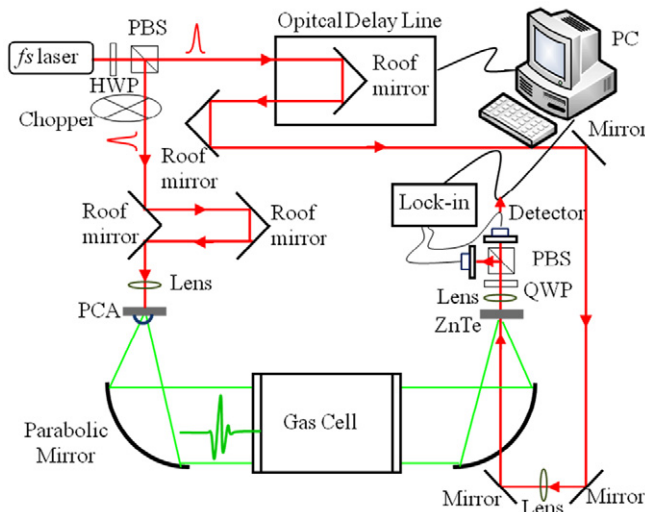
Figure 1. Schematic diagram of a THz spectrometer; HWP: half-wave plate; PBS: polarizing beam splitter; PCA: photoconductive antenna; QWP: quarter-wave plate; ZnTe: zinc telluride crystal.

becomes meaningless because this high accuracy cannot be effectively transferred to an actual measurement. Another problem of calibration with CO gas is the need for enough space for placing the gas cell and a sufficiently long THz beam path for the reaction of THz and CO gas, which limits the application of this technique in compact THz spectrometers and reflection-type THz spectrometers [10].

Naftaly *et al* also described a frequency calibration using an etalon in detail in [6], which can be performed as a stand-alone technique. However, this technique is still unsuitable for on-line calibration. The calibration cannot be performed at the same time as the measurement, because this technique causes an energy loss and an interferential spectrum, which decreases the signal-to-noise ratio (SNR) of the THz spectrometer and makes spectral analysis difficult [11, 12]. There usually exists at least one THz echo pulse in the time-domain waveform in a THz spectrometer, which may be generated from THz emission elements, detection crystals, beam splitters or other optical components [12, 13]. Echo pulses cause spectral interference in the frequency domain after Fourier transform [11, 12]; therefore, a commonly used method to exclude the echo is to keep the scan length just shorter than the first echo [11]. However, we found that the echo is useful in the calibration of THz spectrometers, which can be used as a transfer standard to calibrate THz spectrometers on-line. This calibration technique simplifies the conventional calibration using laser interferometry and causes no performance degradation of the THz spectrometer. The calibration is performed at the same time as specimen measurement, and the linear error of spectrometer repetition can be corrected.

2. THz spectrometer calibration with CO

We fabricated a THz spectrometer, the schematic diagram of which is shown in figure 1. We use a femtosecond laser as a pump source. The pulse is split into two paths; one is used

to pump a photoconductive antenna (PCA) for generation of THz radiation, and the other is used to detect the generated THz focused by a parabolic mirror on an electro-optic (EO) crystal. The THz electric field is detected with a balanced detector placed after a polarizing beam splitter, and the amplitude is read via a lock-in amplifier.

We employed a CO gas cell to calibrate the THz spectrometer. We placed the gas cell in the THz transmission optical path (shown in figure 1), and measured the THz waveform after passing through the gas cell filled with CO gas at a pressure of 2 bar and with vacuum (shown in figure 2(*a*)). The absorption lines of CO gas were deduced and the peaks of the absorption lines were compared with the data reported in the HITRAN database (shown in figure 2(*b*)) [6, 9].

With the calibrated spectrometer, we made eight independent measurements of the CO gas absorption lines with the same gas cell. The results are shown in figure 3.

Figure 3(*a*) depicts the measured THz waveforms and figure 3(*b*) depicts the THz spectra obtained after Fourier transform. From figure 3(*b*), we found that the measured absorption peaks of the same CO gas are not well reproduced for the eight independent measurements. In figure 3(*a*), there is considerable dislocation of the echo peaks. The unrepeatability of the waveforms naturally results in the spectra unrepeatability in figure 3(*b*). The standard deviation of the eight measurements around the 1.04 THz absorption peak is 4.19 GHz. Therefore, a relative uncertainty of 0.4% is generated from the unrepeatability.

3. THz echo pulse and THz spectrum

The unrepeatability of the THz spectrometer makes it impossible for accurate characterization of specimens in the THz region. In THz time-domain spectroscopy (THz-TDS), a complex spectrum is obtained after Fourier transform of the probed THz pulse waveforms [10, 14]. Therefore, we traced the THz spectrum unrepeatability to the THz waveforms. We found that the unrepeatability of the THz spectra originates from the unrepeatability of pulse waveforms (figures 3(*a*) and (*b*)). Therefore, an on-line calibration of the time-domain waveforms is desirable.

A commonly used strategy in a THz spectrometer is the generation of THz radiation with a PCA and detection by EO sampling with a zinc telluride (ZnTe) wafer [10, 11]. In the optical setup in figure 1, we also adopted this scheme and we used 3 mm thick ZnTe as the EO sampling crystal. A THz echo pulse is generated by subsequent reflections from the two interfaces between the ZnTe crystal and air. The delay τ between the main pulse and the echo pulse can be written as

$$\tau = c \cdot n_{\text{THz}} \cdot d \qquad (1)$$

where c is the speed of light in vacuum, n_{THz} is the refractive index of ZnTe in the input THz pulse spectral range and d is the thickness of ZnTe. Figure 4 shows the corresponding THz pulse waveform and its echo pulse. The main pulse occurs at 6 ps and its echo pulse is at 71 ps.

The THz spectrum is obtained with Fourier transform of the THz waveform. If the echo pulse is included, the resultant
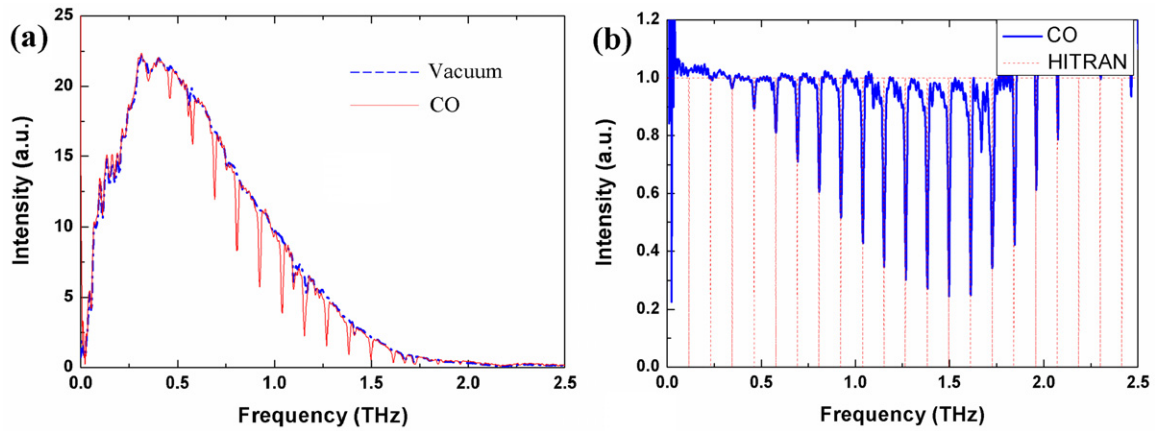
Figure 2. Calibration of the THz spectrometer with CO gas. (*a*) Measured THz spectrum passed through the gas cell with CO gas and that with a vacuum, (*b*) deduced CO absorption lines and the data in the HITRAN database [9].
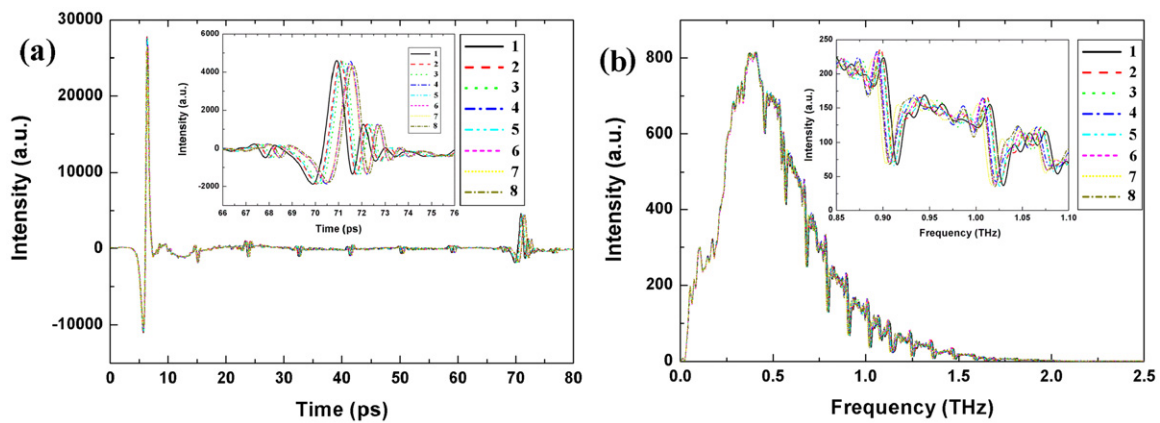

Figure 3. Eight measurements of the THz waveforms and their spectra. (*a*) Measured THz waveforms; inset: magnification of waveforms from 20 ps to 45 ps. (*b*) Fourier-transformed THz spectra obtained with the waveform of 1 ps to 65 ps; inset: magnification of spectra from 0.5 THz to 1.0 THz.
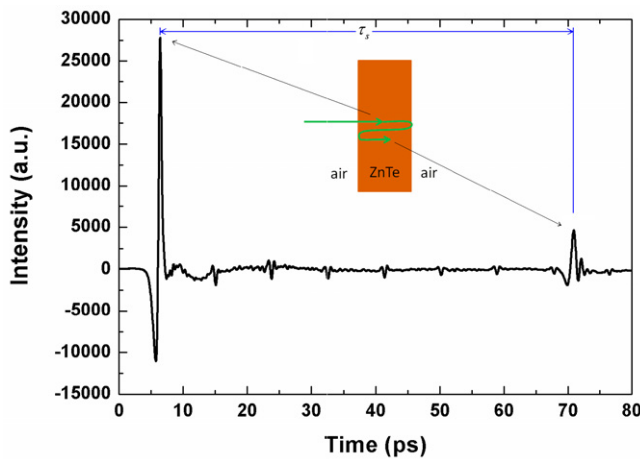

Figure 4. Measured THz waveform with a sweep length of 80 ps. The main pulse occurs at 6 ps and its echo pulse at 71 ps.

spectrum shows interference features [11, 15]. Figure 5(*a*) is a Fourier-transformed spectrum of an 80 ps long waveform. These interference structures hide real spectral features [11]. If the echo pulse is excluded, the interference does not occur and a real spectrum is revealed. Figure 5(*b*) shows a Fourier-

transformed spectrum of a 65 ps long waveform, the echo pulse being excluded.

Therefore, a commonly used method is to keep the scanning length shorter than the first echo. The echo is excluded in the recorded THz waveform. However, with this method one loses the useful information in the echo pulse. In equation (1), there are two factors that determine the delay. One is the refractive index of ZnTe n_{THz} and the other is the thickness of ZnTe d. The refractive index of ZnTe is flat from 0 THz to 3 THz [16]; therefore, the group delay and dispersion are insensitive to the THz spectrum envelope. The thickness of the ZnTe crystal is fixed for a certain spectrometer, and the thermal expansion coefficient of ZnTe at 25 °C is 8.5×10^{-6} °C^{-1} [17]. Therefore, the delay between the main pulse and the echo pulse is a constant, and it can be taken as a standard to calibrate THz spectrometers. In sections 4 and 5, we will demonstrate how to use the echo pulse to calibrate THz spectrometers on-line.

4. Traceability of echo delay to CO absorption lines

We performed a traceable measurement of the standard echo delay to the CO gas absorption lines, and then we used the
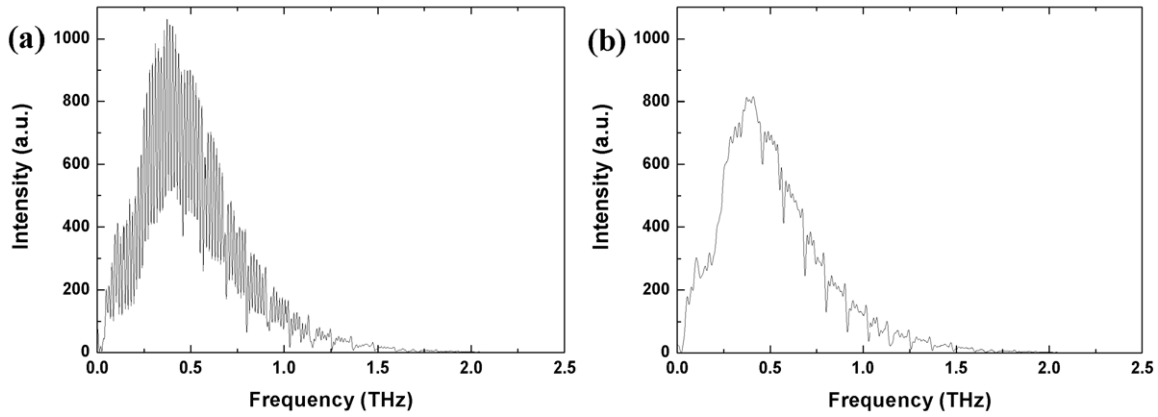
Figure 5. THz spectra of the measured THz waveform obtained with Fourier transform. (*a*) Transformed time length of 80 ps; (*b*) transformed time length of the first 65 ps, wherein the echo pulse is excluded.

standard echo delay to on-line calibrate 'each shot' of the measured THz waveforms. Alternatively, the standard echo delay is also traceable to the etalon [6], or laser interferometry, or the combination of the refractive index of ZnTe n_{THz} and the thickness d in equation (1). We compared the measured absorption peaks of CO gas in figure 5(*b*) with the HITRAN database [9]. We took the HITRAN database as a reference, and a correction coefficient of this calibration was calculated from

$$C_f = \frac{f_{p,\,s}}{f_{p,\,m}} \qquad (2)$$

where $f_{p,\,m}$ is the measured absorption peak of CO gas, and $f_{p,\,s}$ is the corresponding one in the HITRAN database. We compared ten absorption peaks and used the average of these ten correction coefficients as the final correction factor. The measured absorption peaks of CO gas and those of the HITRAN database are listed in table 1. With the result in table 1, the frequency axis should be multiplied by a correction factor of 1.004 75. Table 1 also gives the standard deviation of the ten correction coefficients. The calculated relative standard deviation is 0.13%.

Based on the theory of Fourier transform, the corresponding time-domain waveform should be divided by the same correction factor, if the frequency spectrum has been multiplied by a correction factor. This relationship can be expressed as

$$\left. \begin{array}{c} f(t) \Leftrightarrow \tilde{F}(\omega) \\ f\left(\frac{t}{C_f}\right) \Leftrightarrow \tilde{F}(C_f \cdot \omega) \end{array} \right\} \qquad (3)$$

where $\tilde{F}(\omega)$ is the Fourier transform of a time-domain function $f(t)$, and C_f is the frequency correction factor.

Based on equation (3), the time axis in figure 4 should be divided by the same correction factor of 1.004 75 correspondingly. Therefore, the standard delay between the main pulse and the echo τ_s can be corrected with

$$\tau_s = \frac{\tau_m}{C_f}. \qquad (4)$$

Here τ_m is the originally measured echo delay. The originally measured echo delay in figure 4 is 64.500 ps. Therefore, the

Table 1. Measured absorption peaks of CO and those in the HITRAN database [9].

Measured peaks/THz	HITRAN database/THz	Correction coefficient
0.458	0.461	1.006 55
0.572	0.576	1.006 99
0.684	0.691	1.010 23
0.801	0.807	1.007 49
0.915	0.922	1.007 65
1.029	1.037	1.007 77
1.146	1.152	1.005 24
1.258	1.267	1.007 15
1.372	1.382	1.007 29
1.485	1.497	1.008 08
Average		1.007 45
Standard deviation		0.001 26

corrected echo delay is 64.023 ps. The sampling time of the waveform is 0.038 ps; therefore, the uncertainty component is $0.038/2\sqrt{3} = 0.011$ ps with a rectangular probability distribution [18]. The relative standard uncertainty component is 0.017% ($k = 1$). This corrected delay of 64.023 ps can be taken as a transfer standard for on-line calibration of THz waveforms, because it is a constant at a certain temperature for a certain spectral envelope. The echo is generated by reflection between the two interfaces of ZnTe and air. The coefficient of expansion of ZnTe is $8.5 \times 10^{-6}\,°C^{-1}$ [17]. Therefore, the relative uncertainty component is $8.5 \times 10^{-6}/\sqrt{2} = 0.0006\%$ with an arcsine probability distribution ($k = 1$) for the surrounding temperature varying within $\pm 1\,°C$ [18].

5. On-line calibration with standard echo delay

We use the standard echo delay of 64.023 ps to calibrate each 'shot' of the previously measured THz waveforms in figure 3(*a*). The calibrated waveforms are shown in figure 6(*a*). In comparison with figure 3(*a*), the agreement in figure 6(*a*) of the eight measurements is remarkably improved. The peaks of the echo coincide with each other perfectly after this on-line correction.
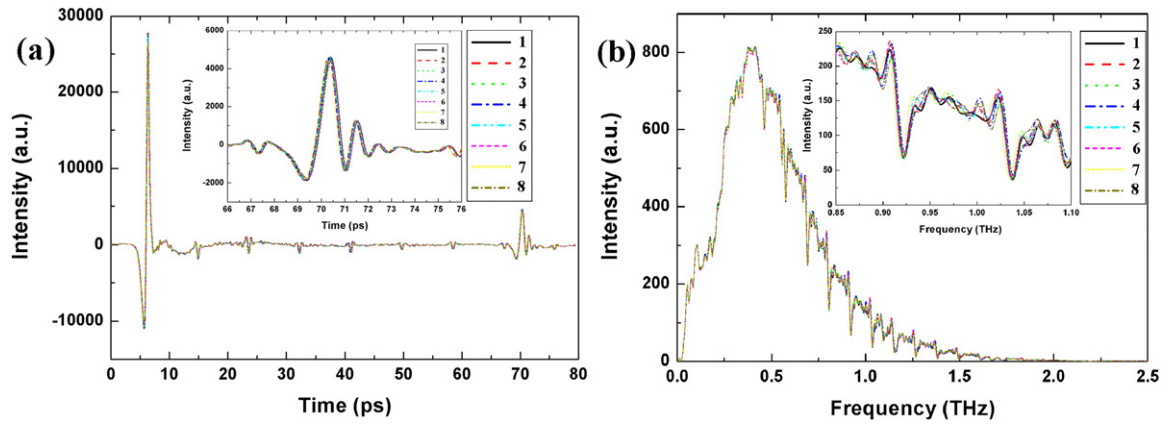
Figure 6. Calibrated THz waveforms and spectra with the standard echo delay. (*a*) Calibrated THz waveforms with the standard echo delay; inset: magnification of calibrated echo waveforms from 66 ps to 76 ps. (*b*) Fourier transform of the calibrated THz waveforms with the standard echo delay; inset: magnification from 0.5 THz to 1.0 THz.
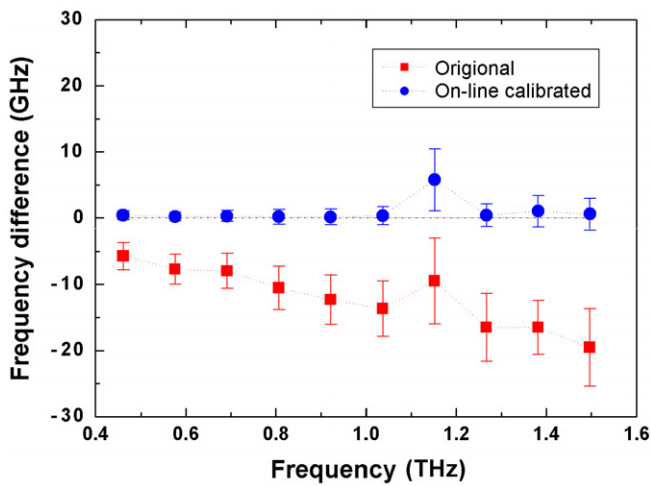

Figure 7. Comparison of the measured absorption peaks with those in the HITRAN database. The red solid squares and the blue solid points represent the difference of the originally measured absorption peaks of CO gas and the calibrated ones from those reported in the HITRAN database, respectively.

Although the waveforms are recorded including the echo pulse, the effective spectra can be obtained by applying a rectangular filter window to the time-domain trace to exclude the echo for removal of spectral interference. The transformed spectra with a filter window of 0 ps to 65 ps are shown in figure 6(*b*). On comparison with figure 3(*b*), it is seen that the repeatability in figure 6(*b*) is significantly improved. The absorption peaks agree with each other very well after this on-line calibration operation.

6. Uncertainty analysis and discussion

We extracted the absorption peaks of the originally measured spectra and those of the calibrated ones. Their differences with the referred value in the HITRAN database [9] are shown in figure 7. The red solid squares and the blue solid points represent the difference of the originally measured absorption peaks of CO gas and the calibrated ones from those reported in the HITRAN database, respectively. The error bars are the standard deviation of the eight measurements.

Table 2. Uncertainty budget of THz spectrometer calibration with echo pulse.

Uncertainty source	Distribution	Type	Relative uncertainty
Traceability to CO absorption lines	Normal	A	0.13%
Time resolution of the THz waveform	Rectangular	A	0.017%
Temperature coefficient of expansion	Arcsine	A	0.0006%
THz spectral envelope	Normal	B	0.05%
Repetition of the THz spectrometer	Normal	A	0.166%
Combined uncertainty	Normal		0.22% ($k = 1$)

In figure 7, the original measurement results deviate from the standard values. However, the on-line calibrated ones fully agree with the reference values. This demonstrates that the irregular unrepeatability results in a great deviation. With the echo on-line calibration operation, the unrepeatability is effectively corrected. Each 'shot' of the measurement waveform is referred to the standard echo delay and accurate measurement results are obtained.

Moreover, with this on-line calibration, the measurement uncertainty is reduced. Figure 7 shows that the frequency differences are caused by a systematic frequency error, which increases linearly with frequency and not by random uncertainties. Therefore, we use a relative value to evaluate the standard deviation. The relative standard deviation of the original measurement results is 0.415%, and that of the on-line calibrated results is 0.166%. Therefore, the measurement standard deviation is 2.5 times as small as the original one.

In figure 7, both the original results and the on-line calibrated ones show a large deviation around 1.152 THz. This is because water vapour has an absorption peak in the neighbourhood of this frequency point [7]. Although the THz waveforms were measured under ambient dry air, the residual water vapour influenced the measurement results at this frequency point.

An uncertainty budget is summarized in table 2. It is worth noting that the echo pulse is generated inside the ZnTe wafer.
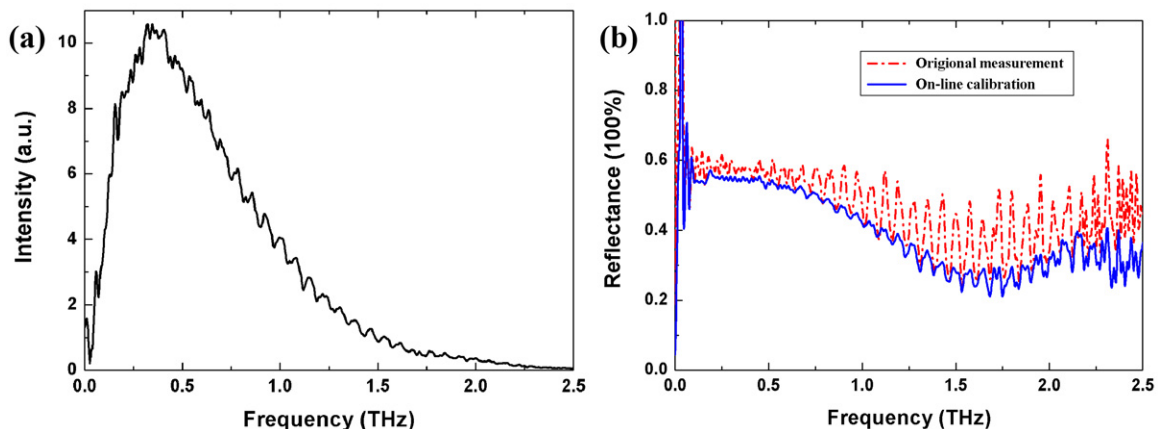
Figure 8. SiC reflectance measurement with a rippled THz spectrometer. (*a*) Rippled background spectrum, (*b*) measured reflectance of SiC; the red dashed and dotted line is the original measurement and the blue solid line the on-line calibrated result.

The echo delay is immune to the water vapour. However, the water vapour outside the wafer modifies the THz spectral envelope; the group delay is therefore varied. Fortunately, the index of refraction of ZnTe is flat in the 0 THz to 3 THz range [16]. We evaluate a 0.05% relative uncertainty for the effect of group delay.

This on-line calibration technique is also effective for measurement with rippled THz spectrometers. Figure 8(*a*) is a measured rippled THz spectrum with a THz spectrometer in reflection geometry [10]. The ripple may be generated from some reflectance of optical elements. We measured the spectral reflectance of a silicon carbide (SiC) wafer. The original measurement is shown in figure 8(*b*) with a red dashed and dotted line. Due to frequency errors of the spectrum of the specimen and that of the reference one, the dislocation of the two spectra in frequency causes large fluctuations of the measured spectral reflectance profile. There is not sufficient space to place a CO gas cell in reflection-type THz spectrometers for calibration. Using an etalon may introduce an interferometric spectrum. Moreover, both of the calibration techniques are unsuitable for on-line calibration. However, with this echo calibration technique, the fluctuation is greatly reduced and accurate spectral reflectance can be obtained. The on-line calibration result is shown in figure 8(*b*) with a blue solid line.

As mentioned above, an echo pulse can also be generated from beam splitters, lenses or other optical elements [11, 13]. If there are no suitable echoes available, one can embed a thick silicon plate. The THz pulse makes a round trip between the two interfaces of silicon and air, and then an echo is generated. However, the frequency resolution may be limited by the thickness of the silicon plate, and the amplitude of the waveform may be reduced by reflection of the silicon surface.

The single 'shot' mentioned above is a quasi-single shot. It means each measurement can be corrected using the measured data itself. The ultrafast pulse waveform is obtained with EO sampling or PC sampling; it cannot be recorded in an absolutely single shot.

The calibration of the time axis of a THz spectrometer can also be carried out with a laser interferometer; however, this echo delay calibration is easier and more effective than laser interferometry.

7. Conclusion

We take the delay between the main pulse and the echo pulse as a standard to perform on-line calibration of a THz spectrometer for correction of linear time-base errors. The echo delay is traceable to the CO gas absorption lines reported in the HITRAN database, and then it is used as a transfer standard to calibrate each 'shot' of the measured THz waveforms. With this embedded on-line calibration, the deviation generated from the unrepeatability is effectively corrected, and the relative standard deviation is reduced by a factor of 2.5. This embedded on-line calibration transfers the uncertainty to actual measurement effectively, because the calibration is carried out at the same time in each measurement. This calibration needs no additional optical components and causes no performance degradation of the THz spectrometers. This echo calibration technique significantly reduces the fluctuation caused by the rippled reference spectrum. It effectively links the standard and the actual measurement. With this calibration technique, spectral properties of a specimen can be precisely characterized in the THz region even with an unrepeatable THz spectrometer. It is effective in actual applications on accurate characterization of the spectral properties of specimens in the terahertz region.

With this technique, the linear error of delay time can be corrected. It provides an alternative technique traceable to the International System of Units (SI).

Acknowledgments

References

[1] Ferguson B and Zhang X-C 2002 Materials for terahertz science and technology *Nature Mater.* **1** 26–33

[2] Tonouchi M 2007 Cutting-edge terahertz technology *Nature Photon.* **1** 97–105

[3] Takayanagi J, Kanamori S, Suizu K, Yamashita M, Ouchi T, Kasai S, Ohtake H, Uchida H, Nishizawa N and Kawase K 2008 Generation and detection of broadband coherent terahertz radiation using 17 fs ultrashort pulse fiber laser *Opt. Express* **16** 12859–65

[4] Xiong W and Shen J 2010 Fingerprint extraction from interference destruction terahertz spectrum *Opt. Express* **18** 21798–803

[5] van Exter M P, Fattinger Ch and Grischkowsky D 1989 Terahertz time-domain spectroscopy of water vapor *Opt. Lett.* **14** 1128–30

[6] Naftaly M, Dudley R A, Fletcher J R, Bernard F, Thomson C and Tian Z 2009 Frequency calibration of terahertz time-domain spectrometers *J. Opt. Soc. Am.* B **26** 1357–92

[7] Cheville R A and Grischkowsky D 1999 Far-infrared foreign and self-broadened rotational linewidths of high-temperature water vapor *J. Opt. Soc. Am.* B **16** 317–22

[8] Xin X, Altan H, Saint A, Matten D and Alfano R R 2006 Terahertz absorption spectrum of para and ortho water vapors at different humidities at room temperature *J. Appl. Phys.* **100** 094905

[9] Rothman L S *et al* 2005 The HITRAN 2004 molecular spectroscopic database *J. Quant. Spectrosc. Radiat. Transfer* **96** 139–204

[10] Deng Y, Sun Q, Yu J, Lin Y and Wang J 2013 Broadband high-absorbance coating for terahertz radiometry *Opt. Express* **21** 5737–42

[11] Zomega Terahertz Corporation 2012 *The Terahertz Wave eBook* http://dl.z-thz.com/eBook/zomega_ebook_pdf_1206_sr.pdf

[12] Pupeza I, Wilk R and Koch M 2007 Highly accurate optical material parameter determination with THz time-domain spectroscopy *Opt. Express* **15** 4335–50

[13] Bieler M and Füser H 2013 Realization of an ultra-broadband voltage pulse standard utilizing time-domain optoelectronic techniques *Proc. SPIE* **8624** 862417

[14] Grischkowsky D, Keiding S R, van Exter M and Fattinger Ch 1990 Far-infrared time-domain spectroscopy with terahertz beams of dielectrics and semiconductors *J. Opt. Soc. Am.* B **7** 2006–15

[15] Sun Q, Deng Y, Cao S, Yu J, Liu F, Wang C and Xing Q 2010 Joint time–frequency analysis for terahertz time-domain spectroscopy *Spectrosc. Spectr. Anal.* **30** 3169–73 (in Chinese)

[16] Gallot G, Zhang J, McGowan R W, Jeon T and Grischkowsky D 1999 Measurements of the THz absorption and dispersion of ZnTe and their relevance to the electro-optic detection of THz radiation *Appl. Phys. Lett.* **74** 3450–2

[17] Holland H J and Beck K 1968 Thermal expansion of zinc telluride from 0° to 460 °C *J. Appl. Phys.* **39** 3498–9

[18] BIPM, IEC, IFCC, ILAC, ISO, IUPAC, IUPAP and OIML 2008 *Evaluation of Measurement Data—Guide to the Expression of Uncertainty in Measurement* JCGM 100:2008